MINIMIZATION OF NONLINEAR EFFECTS OF INSERTION DEVICES AT SPS STORAGE RING*

P. Sunwong†, P. Sudmuang, T. Pulampong[1], S. Krainara, S. Kongtawong, P. Klysubun
Synchrotron Light Research Institute, Nakhon Ratchasima, Thailand
[1]also at John Adams Institute for Accelerator Science, Oxford, UK

Abstract

Nonlinear effects of insertion devices were studied for the Siam Photon Source (SPS) storage ring. Despite the fact that shimming technique was used to minimize the nonlinear components of magnetic field integral arising from random errors, the nonlinear dynamics effects still remain. It was found that calculated dynamic field integrals are largest in the 2.2 T Hybrid Multipole Wiggler (MPW). Dynamics effects of insertion devices are attributed to the wiggling trajectory of electron in the region of magnetic field roll-off due to finite pole width. For better and more effective operation of the SPS storage ring, multipole components of the dynamic field integral in the MPW have to be further reduced.

INTRODUCTION

Three insertion devices (IDs), namely, a 0.55 T Undulator (U60), a 2.2 T Hybrid Multipole Wiggler (MPW) and a 6.5 T Superconducting Wavelength Shifter (SWLS), have been installed and operated in the Siam Photon Source (SPS) storage ring. Linear effects of the IDs such as vertical focusing (edge focusing) were studied using hard-edge model and successfully compensated by optical matching using MAD-X code [1]. Nevertheless, nonlinear effects due to higher-order multipole field components produced by IDs can also have large impacts on electron beam dynamics, such as a significant reduction in dynamic aperture [2]. In the case of SPEAR BL11 wiggler, for example, the dynamic aperture was drastically reduced due to nonlinear perturbation from magnetic field roll-off associated with the finite wiggler pole width [3]. The nonlinear fields in SPEAR wiggler were characterized by calculations of dynamic field integral. In the case of the SPS 2.2 T MPW, the pole width is 70 mm, and the minimum gap is 23.5 mm. The good field region of MPW is ±5 mm where $\Delta B/B < 0.1\%$. This multipole wiggler was originally designed for Synchrotron Radiation Source (SRS) with the peak field of 2.4 T at 20 mm pole gap [4]. Shimming technique was used before MPW installation to reduce the nonlinear field integral from random errors. It was found that nonlinear effects of the 2.2 T MPW are still large among the three IDs, which results in a considerable decrease in dynamic aperture [5]. Electron beam injection into the SPS storage ring when the MPW gap is closed is also difficult. These are attributed to the nonlinear terms of dynamic field integral similar to the case of SPEAR wiggler.

MEASUREMENT OF FIELD INTEGRAL AND CORRECTION

Before installation of SWLS and MPW in the SPS storage ring, the field integrals due to random errors were measured using flipping coil technique. The random errors are from construction tolerances such as the pole misalignment and displacement. Figure 1 presents the measured field integrals for SWLS operated at 6.5 T and MPW operated at 2.4 T. Dashed lines are polynomial fits to the data with the resulting polynomial coefficients listed in Table 1.

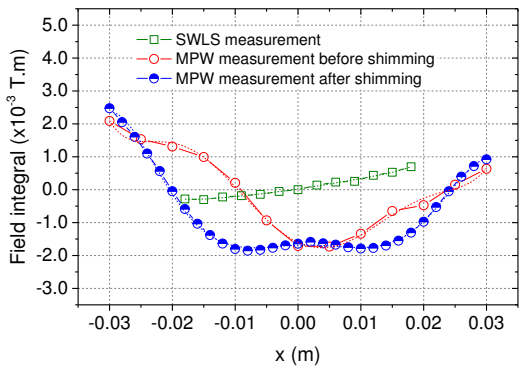

Figure 1: Measured field integrals of SWLS and MPW at the peak field of 6.5 T and 2.4 T, respectively.

It was found that quadrupole components of the field integrals are comparable between SWLS and MPW but nonlinear sextupole component of MPW is much higher than that of SWLS. In general, linear effects of the integrated quadrupole component on electron beam can be reduced by optics correction during commissioning process. In our case, the SWLS is installed in the middle of a straight section, therefore an effective correction can be achieved relatively easily [1]. Nonlinear effects of the integrated sextupole component, on the other hand, can be reduced by shimming technique. A set of magnetic shims were placed on top of the 1st, 3rd, 5th, 7th and 9th poles of MPW at x = -10 mm and x = 15 mm to reduce the sextupole component. The shim's dimension is 15 mm × 10 mm. The shim's thickness is 0.43 mm for shims placed at x = -10 mm and 0.20 mm for shims placed at x =15 mm. Measured field integral of MPW after shimming process is also plotted in Fig. 1. The integrated sextupole component was reduced from 11 T/m to -2 T/m. The remaining quadrupole integral was 6.4×10^{-3} T.

* Work supported by Synchrotron Light Research Institute, Thailand.
† prapaiwan@slri.or.th

ISBN 978-3-95450-147-2

Copyright © 2016 CC-BY-3.0 and by the respective authors

Table 1: Measured Multipole Integral

Terms	SWLS	MPW before shimming	MPW after shimming
x^0	2.2×10^{-5}	-1.6×10^{-3}	-1.7×10^{-3}
x^1	2.8×10^{-2}	-8.7×10^{-2}	6.4×10^{-3}
x^2	5.5×10^{-1}	1.1×10^{1}	-2.0×10^{0}
x^3	-9.8×10^{0}	1.5×10^{2}	-9.5×10^{1}
x^4	-1.5×10^{3}	-2.0×10^{4}	1.7×10^{4}
x^5	2.3×10^{4}	-8.6×10^{4}	6.8×10^{4}

DYNAMIC FIELD INTEGRAL

Dynamics effects of a wiggler on electron beam arise from wiggling trajectory of the electron itself. As such the effects come up even for the case of an ideal wiggler. Finite pole width creates magnetic field roll-off in horizontal direction, so the wiggled electron may experience the field that consists of linear and nonlinear multipole components. The so-called dynamic field integral along electron trajectory is used to characterize dynamic effects of IDs similar to the way that static field integral (from flipping coil measurement) is used to analyse the field error effects.

Kick Map Method

In general approach to electron beam dynamics, the field components are expanded about electron trajectory in the equations of motion and the second-order angular deflections or dynamic kicks are obtained [6]. The kick map method has been used to model and study dynamic effects of IDs [7-9]. Elleaume's kick map is derived from the two dimensional potential function $\Psi(x,y)$ and the kicks can be calculated with RADIA magnetostatic code. Magnetic field of the ID is assumed to be periodic along z-coordinate and expanded into Fourier series with $B_1 >> B_n$ for $n > 1$. Horizontal and vertical kicks are then computed as a function of electron beam transverse position in xy-plane at entrance of the ID. The horizontal deflection due to dynamic effects is given by:

$$\Delta x' = -\frac{1}{2}\frac{L}{(B\rho)^2}\left(\frac{\lambda}{2\pi}\right)^2 B_y \frac{dB_y}{dx}. \qquad (1)$$

L and λ are the total length and the period length of the wiggler, respectively. This horizontal kick can be written in terms of dynamic field integral along the wiggling trajectory (s) as $\Delta x' = (1/B\rho)\int B_y ds$. The vertical kick ($\Delta y'$) can be derived in a similar way. Figure 2 shows kick maps of the IDs calculated using RADIA code. The kicks are presented in the unit of T^2m^2, independent of electron energy. It can be seen that magnetic field of U60 undulator hardly change the angle of traversing electron. Peak field of U60 is 0.55 T and the calculated good field region is ±6 mm at $\Delta B/B < 0.1\%$. Despite a small good field region, the low field of U60 results in negligible effect on the horizontal electron beam dynamics.

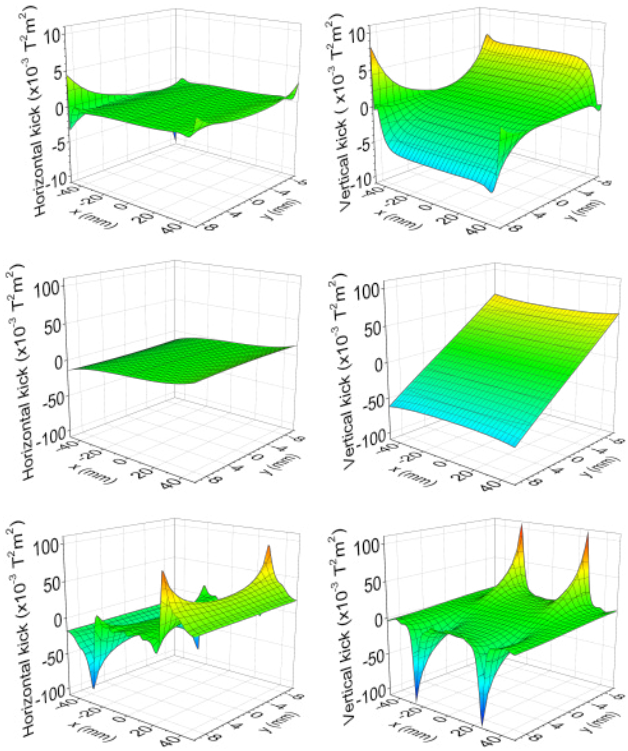

Figure 2: Calculated horizontal and vertical kick maps of U60 (top), SWLS (middle) and MPW (bottom) at the peak field of 0.55 T, 6.5 T and 2.2 T, respectively.

For high-field IDs such as SWLS and MPW, the kicks are larger than that of U60 in both directions. The kick angle is not only dependent on the magnitude and quality of the magnetic field, but also increasing with the number of magnetic periods. It is worth noting that the vertical kick obtained from dynamics analysis here is the vertical focusing characterized in the hard-edge model. It increases linearly with vertical position near the vertical mid-plane and is a second-order effect. Main characteristics of the three IDs in the SPS storage ring are summarized in Table 2. For the MPW, the small good field region clearly arises from the narrow pole width that makes the field to roll off quickly at $x = \pm5$ mm, as illustrated in Fig. 3. Also plotted in the figure is the horizontal kick of IDs taken from kick map at $y = 0$ which demonstrates the relation between the kick, the magnetic field and the field roll-off given by Eq. (1).

Table 2: Insertion Devices in SPS Storage Ring

Parameters	U60	SWLS	MPW
Peak field (T)	0.55	6.5	2.2
Number of main poles	80	1	9
Pole width (mm)	96	139	70
Good field region (mm) $\Delta B/B < 0.1\%$	±6	±15	±5
Measured tune shift			
horizontal	-	-0.040	-0.024
vertical	-	0.106	0.037

Copyright © 2016 CC-BY-3.0 and by the respective authors

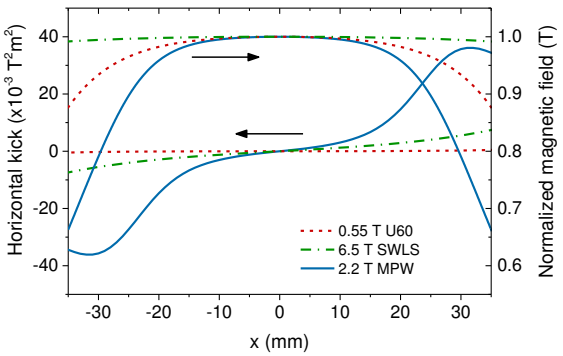

Figure 3: Calculated horizontal kick and normalized magnetic field of insertion devices as a function of x.

Tune Measurements

Tune measurements were performed for different operation modes of the SPS storage ring to investigate the effects of the IDs. The measured tune shift from SWLS and MPW operations is included in Table 2. For SWLS, no field correction was applied and the quadrupole component is 2.8×10^{-2} T from the measured field integral and 2.9×10^{-2} T derived from Fig. 3. On the other hand, the measured quadrupole integral of MPW after shimming is 6.4×10^{-3} T while it is 7.4×10^{-3} T from calculated dynamic field integral. These values explain the larger horizontal tune shift in SWLS since the betatron functions at the two IDs are not significantly different. Tune shift was also observed with closed orbit bump in SWLS and MPW. Details of tune measurements and complete measurement results are reported elsewhere [5]. Figure 4 shows measured tune shifts for MPW as a function of the pole gap, in comparison with simulations using hard-edge model and kick map using ELEGANT code.

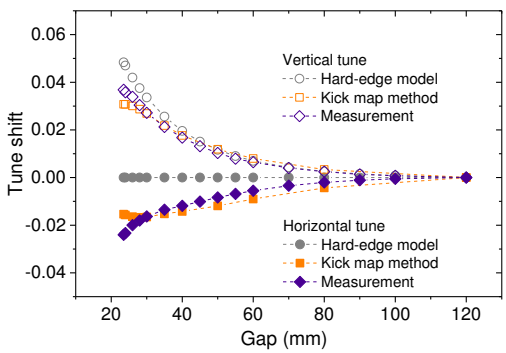

Figure 4: Tune shift at various gaps of MPW.

The hard-edge model predicts vertical tune shift due to vertical focusing rather well, although its infinite pole width assumption fails to explain horizontal tune change. Difference between horizontal tune shifts from kick map method and from measurements is explained by the remaining field integral after shimming, which is gap-dependent. Anomalous decrease in tune shift estimated from kick map method at low gap is preliminarily from the field computation in RADIA. More detailed study is needed in order to verify the results.

Minimization of Dynamic Field Integral

It can be seen from dynamics analysis that nonlinear effect of MPW from the field roll-off is large and should be of concern. It was also found from tracking in ELEGANT that the dynamic aperture is reduced by more than 75% by the operation of MPW [5]. Dynamic field integral may be compensated using several techniques such as L-shaped shims, active shimming, and magic fingers [3, 10-11]. Dynamic multipole integral of MPW derived from Fig. 3 for -30 mm $\le x \le$ 30 mm can be described by $\int B_y ds = -2.6\times10^{5}\, x^5 + 1.3\times10^{-3}\, x^4 + 5.7\times10^{2}\, x^3 - 1.3\times10^{-6}\, x^2 + 7.4\times10^{-3}\, x + 2.7\times10^{-10}$. The integral is dominated by x, x^3 and x^5 terms which are corresponding to 4-pole, 8-pole and 12-pole components, respectively. These multipole components, especially the nonlinear x^3 and x^5 terms, are larger than that of the measured integrals and should be cancelled by the use of magic fingers. Integrated field of the magic fingers can be estimated using the integral of thin lens multipole [3].

CONCLUSION

Magnetic field roll-off in MPW is the primary cause of nonlinear effects on beam dynamics at the SPS storage ring. Nonlinear beam dynamics was characterized using kick map method and calculation of dynamic field integral. With a concern about the reduction of dynamic aperture, correction with magic fingers will be implemented. Future work will be to optimize geometry and structure of the magic fingers to reduce the x, x^3 and x^5 terms of MPW field integral. Applicability of the magic finger correction will be confirmed by tracking simulation, tune measurements, and observation of the beam lifetime.

REFERENCES

[1] P. Sudmuang *et al.*, in *Proc. IPAC'14*, pp. 1192-1194.

[2] J. A. Clarke, *The Science and Technology of Undulators and Wigglers.* New York, NY, USA: Oxford University Press, 2004.

[3] J. Safranek *et al.*, "Nonlinear dynamics in a SPEAR wiggler", *Phy. Rev. ST Accel. Beams.*, vol. 5, p. 010701, 2002.

[4] M. Cianci *et al.*, "A high-throughput structural biology/proteomics beamline at the SRS on a new multipole wiggler", *J. Synch. Rad.*, vol. 12, p. 455, 2005.

[5] S. Krainara *et al.*, "Analysis of Nonlinear Effects for IDs at the SPS Storage Ring", presented at IPAC'16, Busan, Korea, May 2016, this conference.

[6] P. Elleaume, in *Proc. EPAC'92*, pp. 661-663.

[7] B. Singh, A. Baldwin, R. Bartolini, and I. P. Martin, in *Proc. EPAC'06*, pp. 2092-2094.

[8] H. C. Chao, H. P. Chang, H. J. Tsai, and C. C. Kuo, in *Proc. IPAC'10*, pp. 4578-4580.

[9] E. Wallén and S. C. Leemann, in *Proc. PAC'11*, pp. 1262-1264.

[10] J. Chavanne, P. Elleaume, T. F. Günzel, and P. Van Vaerenbergh, in *Proc. EPAC'2000*, pp. 2346-2348.

[11] B. Singh *et al.*, in *Proc. IPAC'13*, pp. 1997-1999.

Copyright © 2016 CC-BY-3.0 and by the respective authors